Alexandria Engineering Journal (2023) 68, 29–38

HOSTED BY

Alexandria University

Alexandria Engineering Journal

www.elsevier.com/locate/aej
www.sciencedirect.com

ORIGINAL ARTICLE

Stagnation point hybrid nanofluid flow past a stretching/shrinking sheet driven by Arrhenius kinetics and radiation effect

Nurul Amira Zainal [a,*], Iskandar Waini [a], Najiyah Safwa Khashi'ie [a], Abdul Rahman Mohd Kasim [b], Kohilavani Naganthran [c], Roslinda Nazar [d], Ioan Pop [e]

[a] *Fakulti Teknologi Kejuruteraan Mekanikal dan Pembuatan, Universiti Teknikal Malaysia Melaka, Hang Tuah Jaya, 76100 Durian Tunggal, Melaka, Malaysia*
[b] *Centre for Mathematical Sciences, Universiti Malaysia Pahang, Lebuhraya Persiaran Tun Khalil Yaakob, 26300 Gambang Pahang, Malaysia*
[c] *Institute of Mathematical Sciences, Faculty of Science, Universiti Malaya, Kuala Lumpur 50603, Malaysia*
[d] *Department of Mathematical Sciences, Faculty of Science and Technology, Universiti Kebangsaan Malaysia, 43600 UKM, Bangi, Selangor, Malaysia*
[e] *Department of Mathematics, Babeşß-Bolyai University, 400084 Cluj-Napoca, Romania*

Received 29 August 2022; revised 9 December 2022; accepted 2 January 2023
Available online 11 January 2023

KEYWORDS

Arrhenius kinetics;
Stagnation-point flow;
Hybrid nanofluid;
Thermal radiation;
Stretching/shrinking sheet

Abstract The exclusive behaviour of hybrid nanofluid has been actively emphasized due to the determination of improved thermal efficiency. Therefore, the aim of this study is to highlight the stagnation point Al_2O_3-Cu/H_2O hybrid nanofluid flow with the influence of Arrhenius kinetics and thermal radiation over a stretching/shrinking sheet. This particular work is distinctive because it presents a novel hybrid nanofluid mathematical model that takes into account the highlighted issue with a combination of multiple consequences that have not yet been addressed in prior literature. The bvp4c package embedded in MATLAB software is used to address the formulated ordinary differential equations and specified boundary conditions based on similarity solutions. The flow is assumed to be incompressible and laminar, and the hybrid nanofluid is made up of two different types of nanoparticles. The findings demonstrate the viability of dual solutions within the defined ranges of the physical parameters. As predicted, the hybrid nanofluid flow has been convincingly proved to enhance the skin friction coefficient and the heat transfer performance as opposed to viscous flow and nanofluid flow. The heat of reaction and radiation parameters also act as contributing factors in the progress of thermal enhancement. On the other hand, the reaction

* Corresponding author at: Fakulti Teknologi Kejuruteraan Mekanikal dan Pembuatan, Universiti Teknikal Malaysia Melaka, Hang Tuah Jaya, Durian Tunggal, 76100 Melaka, Malaysia.
E-mail address: nurulamira@utem.edu.my (N.A. Zainal).

Peer review under responsibility of Faculty of Engineering, Alexandria University.

https://doi.org/10.1016/j.aej.2023.01.005

rate parameter unexpectedly displays a decreasing trend in the heat transfer rate of the current study. It is anticipated that this study will benefit future research into this potential heat transfer fluid, particularly in the areas of thermal systems and boundary layer analysis.

1. Introduction

The fluid movement near a solid surface's stagnation area is referred to as stagnation point flow. The stagnation flows occur in a variety of application fields, such as submarines, aircraft, and flows over the tips of rockets. The concern of stagnation point flow has been expanded in a variety of approaches, including boundary layer. Historically, Hiemenz [1] started the investigation of stagnation point flow by transforming the Navier-Stokes equations into an ordinary differential equation using the similarity variables. Following that, Eckert [2] extended the proposed formulation by incorporating the momentum and energy equation. Since then, many researchers have extensively investigated the stagnation point flow in various aspects. Dash et al. [3] introduced the numerical approach of stagnation point flow towards a stretching/shrinking surface in the boundary layer using the shooting method. According to Farooq et al. [4], the radiation parameter favors the thermal progression in their investigation towards the radiation impacts of viscoelastic nanofluid in stagnation point flow. In another study, Rostami et al. [5] declared a dual solution in mixed convective stagnation flow by considering a hybrid nanofluids. It is notable that their research concluded that hybrid nanofluids had a higher heat transfer rate than ordinary nanofluids. Khan et al. [6] discussed the heat transfer characteristics in their investigation of the nonlinear nanomaterial in mixed convection flow by utilising the entropy generation. Later, Khan et al. [7,8] scrutinized the flow of two different types of nanofluid with the inclusion of Arrhenius activation energy. It has been noted that the working fluid's flow behaviour has been affected by the activation energy. Javed et al. [9] examined the impact of heat generation/absorption on axisymmetric Casson liquid flow. They concluded that the heat transfer rate decreased as the Casson parameter increased.

In another study, Mahanthesh [10] performed a statistical and exact analysis in a magnetic environment of the $C_2H_6O_2$-H_2O hybrid base fluid. The hybrid nanoliquid flow with quadratic radiation and quadratic Boussinesq approximation is also discussed by Mahanthesh [11–13]. In his series of studies, he found that the rate of heat transfer is more responsive to quadratic radiation. Thriveni and Mahantesh [14] performed a sensitivity analysis of hybrid nanomaterial nonlinear convective heat transfer between two concentrically positioned cylinders with different heat sources. Mackolil and Mahantesh [15] utilized the response surface methodology (RSM) to optimise the thermal Marangoni convective flow of a hybrid nanomaterial's heat transfer rate. Based on their findings, the hybrid nanomaterial is discovered to have improved thermal fields for nanoparticle volume fractions under 2%. Gul et al. [16] inspected the impact of effective Prandtl number in both nanofluid and hybrid nanofluid over a stretching cylinder. Their findings revealed that hybrid nanoliquid temperatures are rising faster than those of ordinary nanoliquids. As a summary, all discoveries mentioned above have been an open field of research in nanofluid technology and heat transfer.

In order to enhance the base fluid's thermophysical properties, working fluids called hybrid nanofluids are made up from a variety of nanoparticles. By adjusting the ratio or concentration of the nanoparticles, one can customise the characteristics of mono nanofluids. Mono nanofluids, on the other hand, demonstrated steady thermophysical properties in a constrained range by using only one type of nanoparticle (metallic or nonmetallic). Hybrid nanofluids have been created in recent years to enhance the features of fluid's thermophysical and heat transfer capabilities. Hybrid nanofluids' hydrothermal properties offer a wide range of uses in heat transfer systems such as heat exchangers, heat sinks, heat pipes, and solar panels. In many applications devices that demand heat transfer, the relationships between the friction factor and the Nusselt number are also listed. In every aspect of human activity, including heating and cooling, generating electricity, manufacturing industries, electronic devices, and biomedical applications depends on the continued expansion and substantial breakthroughs of thermal management. The power density or heat flux has substantially grown due to the component miniaturisation and exponential expansion in manufacturing capabilities, which presents a challenge to the conventional cooling technologies (see the excellent review paper by Muneeshwaran et al. [17]).

According to Huminic and Huminic [18], combining hybrid nanofluid with small channel dimensions of thermal devices makes it possible to obtain appliances with compactness, low thermal resistance, and efficiency. Later, several studies have been conducted to investigate the effectiveness of hybrid nanofluids as heat-transfer fluid in the stagnation point flow. Dinarvand [19] considered copper oxide and silver nanoparticles as hybrid nanofluids to examine the heat transfer in nodal/saddle stagnation-point boundary layer flow problem. He discovered that hybrid nanofluid's thermal properties are better than those of base fluid and nanofluid. Waini et al. [20] observed the behaviour of stagnation boundary layer flow in different geometry which is cylinder and found dual solutions in their exploration studies. Khashi'ie et al. [21] acknowledged that the thermal performance increased as the copper nanoparticle concentration increased in their study of stagnation point flow over a vertical Riga plate. Meanwhile, the unsteady stagnation point flow towards a stretching/shrinking surface featuring hybrid nanofluids has been encountered by Zainal et al. [22,23] in their multiple studies. The above-stated literature proves that hybrid nanofluids may help to intensify the thermal progress in the stagnation point flow. A few more researches on the boundary layer hybrid nanofluid flow and heat transfer are accessible in [24–28].

Heat transfers and boundary layer flow towards a stretching/shrinking sheet has many practical applications in engi-

neering and manufacturing industries. According to Fisher [29], this topic area may also be relevant to polymer technology, where plastic sheets are stretched, and metallurgy, where continuous strips are cooled. Previous research on stretching/shrinking surfaces in the boundary layer and heat transfer is widely available. The study of stagnation point flow across a shrinking sheet was invented by Wang [30]. Bachok et al. [31] discovered that the solutions for a shrinking sheet are not unique, unlike a stretched sheet. The thermal radiation impact on the stagnation region over a stretching/shrinking sheet was investigated by Bhattacharyya and Yalek [32]. Remarkably, the findings show that the heat transfer rate boosts in the first solution due to incorporating the thermal radiation parameter into account. Additionally, these outcomes are consistent with the research done by Waini et al. [33]. Consequently, it is important to note that other governing parameters may change the working fluid behaviour in the boundary layer flow problems.

The thermal radiation impact may alter the temperature distribution in some applications, such as those dealing with dissociating fluids and chemical reactions. This might eventuate in applications such as space vehicle re-entry, astrophysical flows, electrical power generation, and solar power technology [34]. Countless research has examined the effects of radiative and thermal management in nanofluids throughout the years. Elbashbeshy [35] discussed how thermal radiation affects thermal performance along a stretched surface. Waqas et al. [36] completed an analysis of stagnation point flow with radiation and magnetic impact in hybrid nanofluids. They concluded that rising thermal radiation parameters and Eckert numbers cause an increase in the thermal field. Stability and statistical analysis of hybrid nanofluid featuring radiation effect and melting heat transfer are examined by Basir et al. [37]. Their research exposed that the heat transfers via radiation and melting tend to be much higher in hybrid nanofluid, and so does the skin friction coefficient. Asghar et al. [38] examined the influence of thermal radiation in a magnetic environment on three-dimensional flow of hybrid nanofluid. Their findings demonstrated that the radiation parameter values have no effect on the velocity profile. Further analysis of the effects of thermal radiation in hybrid nanofluid flow may be obtained in [39–42].

Analysis of chemical Arrhenius kinetics and activation energy is essential in the diffusion of binary chemical mixes for the movement of species and energy, which will help chemical engineers and scientists in their efforts to stop reaction blowups. The importance of Arrhenius kinetic nanofluid in industrial development is significant to the industrial chemical production, thermal sciences, biomedical device, polymer extrusion, and technological advancement in improving the thermal system [43]. According to Khan et al. [44], the Arrhenius activation energy is the least amount of energy needed to initiate a chemical reaction, based on Arrhenius' pioneering work in 1889. The particles (atoms, molecules) are prepared to participate in chemical reactions once they have obtained this form of energy. Shahid et al. [45] scrutinised the Arrhenius kinetics of bioconvection nanofluid with magnetic impact and they noted that the relative temperature parameter reduces the nanoparticle concentration profile while activation energy optimizes it. Arain et al. [46] performed a numerical analysis on multiphase flow and Arrhenius kinetics in Carreau fluid. Their findings summarised that the reaction rate suppresses the concentration of nanoparticles while activation energy is increased. Shah et al. [47] demonstrated the use of the Arrhenius chemical process on third-grade fluids with temperature-dependent thermo-rheological features in mixed, convective flows, recently. Their research concluded that the concentration profile has been enhanced by the higher activation energy factor.

Prompted by a prior investigation of Merkin and Pop [48], the current study is intended to carefully evaluate the hybrid nanofluid with the combination of alumina and copper nanoparticles subjected to a stagnation point flow. Merkin and Pop [48] only consider viscous flow, while according to recent experimental and numerical studies, nanofluid reacts as a better heat transmission fluid than viscous fluid. Therefore, the primary goal of this study is to widen their field of inquiry by utilising hybrid nanofluid flow with the influence of Arrhenius kinetics, thermal radiation, and heat transfer. In this study, a new hybrid nanofluid mathematical model is presented. By including other influences such as radiation, the current study also intends to address a research gap in the existing literature, especially when it pertains to investigating the stagnation-point hybrid nanofluid flow. As a result, the bvp4c method in the MATLAB package is employed to address this problem. A comparative result has been observed, and a strong connection between previous research and the current results is revealed which leads to the next aim of this study. The final analysis is portrayed in figures and tables form. Overall, it is believed that a thorough investigation of these flows should be strengthened together with the use of mathematical competence considering the importance of stagnation flows in numerous industrial applications. Also, these findings are anticipated to assist other researchers and scientists expand their knowledge of this prospective heat transfer fluid, especially in boundary layer analysis and thermal systems.

2. Mathematical model

We consider the two-dimensional stagnation point flow of a hybrid nanofluid with laminar, steady, and incompressible flows in the boundary layer over a stretching/shrinking surface, as shown in Fig. 1, where x and y are the Cartesian

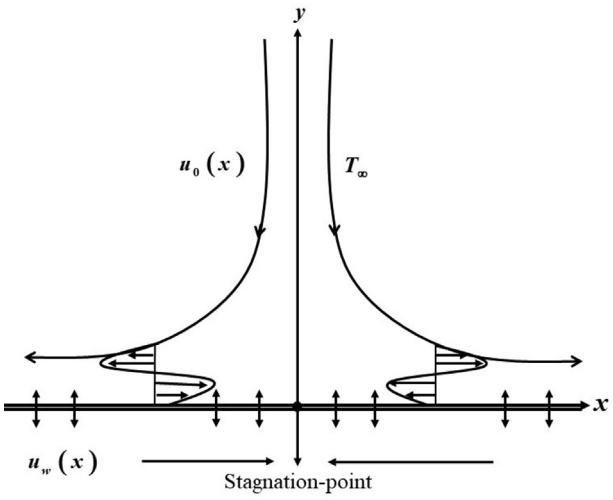

Fig. 1 The physical model.

coordinates with the plate in the plane $y = 0$. It is presumable that Arrhenius kinetics regulate within mass concentration and the fluid temperature on the surface flow. It is also assumed that q_r is the radiative heat flux. In addition, the velocity of the stretching/shrinking sheet is$u_w(x) = (u_e x/l)\lambda$, where u_e is a positive constant, l is a characteristic length of the surface and λ is the stretching/shrinking parameter with $\lambda > 0$ for the stretching sheet, $\lambda < 0$ for the shrinking sheet, and $\lambda = 0$ for the static sheet. The velocity of the far field is denoted as u_0 given that $u_0(x) = u_e x/l$.

As pointed out by Khan et al. [44] in their previous study, the Arrhenius activation energy is the least amount of energy needed to initiate a chemical reaction. Thus, the one-step reaction k regulated by Arrhenius effect is used to illustrate the exothermic surface reaction occurring on the wall by following the work done by Merkin and Pop [48]. Hence, it can be written as

$$A \to B,\ k = \text{rate } k_0 a e^{-E/RT}, \tag{1}$$

where a is the reactant concentration of$A$,B is the product species, E is the activation energy, T is the fluid temperature, k_0 is the rate constant, and R is the gas constant. It is assumed that the base fluid temperature and concentration are T_∞ and a_∞, respectively. It is anticipated that the flow is incompressible and laminar; hence, the governing boundary-layer equations for the assumptions mentioned above can be identified as follows (see Merkin and Pop [48]):

$$\frac{\partial u}{\partial x} + \frac{\partial v}{\partial y} = 0, \tag{2}$$

$$u\frac{\partial u}{\partial x} + v\frac{\partial u}{\partial y} = u_e\frac{du_e}{dx} + \frac{\mu_{hnf}}{\rho_{hnf}}\frac{\partial^2 u}{\partial y^2}, \tag{3}$$

$$u\frac{\partial T}{\partial x} + v\frac{\partial T}{\partial y} = \frac{k_{hnf}}{(\rho C_p)_{hnf}}\frac{\partial^2 T}{\partial y^2} - \frac{1}{(\rho C_p)_{hnf}}\frac{\partial q_r}{\partial y}, \tag{4}$$

$$u\frac{\partial a}{\partial x} + v\frac{\partial a}{\partial y} = D\frac{\partial^2 a}{\partial y^2}, \tag{5}$$

subject to

$$v = 0,\ u = u_w(x),\ k_c\frac{\partial T}{\partial y} = -Qk_0 a e^{-E/RT},$$
$$D\frac{\partial a}{\partial y} = k_0 a e^{-E/RT} \text{ at } y = 0, u \to u_e,\ T \to T_\infty,\ a \to a_\infty \text{ as } y \to \infty. \tag{6}$$

Here u and v are the velocity components along x and y-axes, Q is heat reaction, while D and k_c are the diffusion of mass and thermal conductivity, respectively. We note that μ_{hnf} and ρ_{hnf} are dynamic viscosity and density, respectively, $(\rho C_p)_{hnf}$ is capacity of heat, and k_{hnf} is the heat conductivity. Following that, Table 1 demonstrates the fluids correlations (refer to Takabi and Salehi [49]), and Table 2 displays the properties of ϕ_1 which denotes as Al_2O_3 (alumina) nanoparticle and ϕ_2 signifies the Cu (copper) nanoparticle (see Oztop and Abu-Nada [50]).

We now utilising the Rosseland approximation [51], hence

$$q_r = -\frac{4\sigma^*}{3k^*}\frac{\partial T^4}{\partial y}, \tag{7}$$

where σ^* is the Stefan-Boltzmann and k^* is the coefficient of mean absorption. Now, the temperature differential T^4 in the flow should then be added to Taylor's series. Consequently, by omitting the higher-order expressions and extending T^4 over T_∞ , then

$$T^4 \cong 4T_\infty^3 T - 3T_\infty^4, \tag{8}$$

so that

$$\frac{\partial q_r}{\partial y} = -\frac{16T_\infty^3\sigma^*}{3k^*}\frac{\partial^2 T}{\partial y^2}. \tag{9}$$

Employing Eq. (9) into (43), we have

$$\frac{\partial T}{\partial t} + u\frac{\partial T}{\partial x} + v\frac{\partial T}{\partial y} = \frac{1}{(\rho C_p)_{hnf}}\left(k_{hnf} + \frac{16T_\infty^3\sigma^*}{3k^*}\right)\frac{\partial^2 T}{\partial y^2}. \tag{10}$$

We now introduce the following similarity variables (see Merkin and Pop [48])

$$\psi = x\sqrt{u_e v_f/l}f(\eta),\ \ \eta = y\sqrt{u_e/v_f l},$$
$$T = T_\infty + \left(\frac{RT_\infty^2}{E}\right)\theta(\eta),\ a - a_\infty = a_\infty\chi(\eta). \tag{11}$$

Thus,

$$u = \frac{u_e x}{l}f'(\eta),\ v = -(u_e v_f/l)^{1/2}f(\eta). \tag{12}$$

Substituting the similarity variables (11)-(12) into Eqs. (3), (5) and (10) with boundary conditions (6), we attain:

$$\frac{\mu_{hnf}/\mu_f}{\rho_{hnf}/\rho_f}f''' - f'^2 + f''ff + 1 = 0, \tag{13}$$

$$\frac{1}{\Pr}\left(\frac{1}{(\rho C_p)_{hnf}/(\rho C_p)_f}\right)\left(\frac{k_{hnf}}{k_f} + \frac{4}{3}Rd\right)\theta'' + f\theta' = 0, \tag{14}$$

$$\frac{1}{Sc}\chi'' + f\chi' = 0, \tag{15}$$

$$f(0) = 0,\quad f'(0) = \lambda,$$
$$\theta'(0) = -\alpha(1+\chi(0))e^{\theta(0)/(1+\varepsilon\theta(0))}, \chi'(0) = -\beta(1+\chi(0))e^{\theta(0)/(1+\varepsilon\theta(0))},$$
$$f'(\eta) \to 1,\quad \theta(\eta) \to 0\quad \chi(\eta) \to 0 \text{ as } \eta \to \infty, \tag{16}$$

where primes denote differentiation with respect to η. More definition on the above terms are stated below:

- Pr is the Prandtl number, $\Pr = \frac{(\rho C_p)_f}{k_f}$
- Sc is the Schmidt number, $Sc = \frac{v_f}{D}$
- Rd is the radiation parameter, $Rd = \frac{4\sigma^* T_\infty^3}{(\rho C_p)k_f k^*}$
- α is the chemical reaction rate, $\alpha = \frac{Qk_0 E a_\infty e^{-E/RT}}{k_c RT_\infty^2}\left(\frac{v_f l}{u_e}\right)^{1/2}$
- β is the temperature parameter, $\beta = \frac{k_0 e^{-E/RT}}{D}\left(\frac{v_f l}{u_e}\right)^{1/2}$

However, in order that Eqs. (2) to (5) have similarity solutions, as referred to Merkin and Pop [48], α and β have the form of

$$\alpha = \frac{Qk_0 E a_\infty e^{-E/RT}}{k_c RT_\infty^2}\left(\frac{v_f l}{u_e}\right)^{-1/2}, \beta = \frac{k_0 e^{-E/RT}}{D}\left(\frac{v_f l}{u_e}\right)^{-1/2}. \tag{17}$$

Table 1 Hybrid nanofluid characteristics (Takabi and Salehi [49]).

Characteristics	Alumina-Copper/Water (Al_2O_3–Cu/H_2O)
Dynamic viscosity, μ_{hnf}	$\mu_{hnf}/\mu_f = (1-\phi_{hnf})^{-2.5}$
Heat capacity, $(\rho C_p)_{hnf}$	$(\rho C_p)_{hnf} - (1-\phi_{hnf})(\rho C_p)_f = \phi_1(\rho C_p)_{Al_2O_3} + \phi_2(\rho C_p)_{Cu}$
Density, ρ_{hnf}	$\rho_{hnf} = (1-\phi_{hnf})\rho_f + \phi_1\rho_{Al_2O_3} + \phi_2\rho_{Cu}$
Thermal conductivity, k_{hnf}	$\frac{k_{hnf}}{k_f} = \left[\frac{\left(\frac{\phi_1 k_{Al_2O_3}+\phi_2 k_{Cu}}{\phi_{hnf}}\right)+2k_f+2\left(\phi_1 k_{Al_2O_3}+\phi_2 k_{Cu}\right)-2\phi_{hnf}k_f}{\left(\frac{\phi_1 k_{Al_2O_3}+\phi_2 k_{Cu}}{\phi_{hnf}}\right)+2k_f-\left(\phi_1 k_{Al_2O_3}+\phi_2 k_{Cu}\right)+\phi_{hnf}k_f}\right]$
Electrical conductivity, σ_{hnf}	$\frac{\sigma_{hnf}}{\sigma_f} = \left[\frac{\left(\frac{\phi_1 \sigma_{Al_2O_3}+\phi_2 \sigma_{Cu}}{\phi_{hnf}}\right)+2\sigma_f+2\left(\phi_1 \sigma_{Al_2O_3}+\phi_2 \sigma_{Cu}\right)-2\phi_{hnf}\sigma_f}{\left(\frac{\phi_1 \sigma_{Al_2O_3}+\phi_2 \sigma_{Cu}}{\phi_{hnf}}\right)+2\sigma_f-\left(\phi_1 \sigma_{Al_2O_3}+\phi_2 \sigma_{Cu}\right)+\phi_{hnf}\sigma_f}\right]$

Table 2 The nanoparticles and base fluid properties (Oztop and Abu-Nada [50]).

Characteristics	C_p (J/kgK)	$k\,(W/mK)$	ρ (kg/m^3)
Cu	385	400	8933
Al_2O_3	765	40	3970
H_2O	4179	21	0.613

The coefficient of skin friction C_f, the local Nusselt number Nu_x, including Sh_x which remarks the local Sherwood number, are the physical quantities that are of interest in this work, which is specified as

$$C_f = \frac{\mu_{hnf}}{\rho_f u_e^2}\left(\frac{\partial u}{\partial y}\right)_{y=0},$$
$$Nu_x = \frac{x k_{hnf}}{k_f(T-T_\infty)}\left(\frac{\partial T}{\partial y}\right)_{y=0} + x(q_r)_{y=0},$$
$$Sh_x = -x\left(\frac{\partial a}{\partial y}\right)_{y=0}. \tag{18}$$

Using (11), (12) and (18), we get

$$Re_x^{1/2} C_f = \frac{\mu_{hnf}}{\mu_f} f''(0),\ Re_x^{-1/2} Sh_x = -\chi'(0).$$
$$Re_x^{-1/2} Nu_x = -\left(\frac{k_{hnf}}{k_f} + \frac{4}{3}Rd\right)\theta'(0), \text{where } Re_x = u_e(x)x/\nu_f \tag{19}$$

3. Numerical findings

The results from the bvp4c (MATLAB) solver's computation of Eqs. (13)-(16) for suggested similarity solutions above are documented in this section. The analysis of the flow has been done on both scenarios of stretching ($\lambda > 0$) and shrinking ($\lambda < 0$) cases. Also, it was decided to use relative tolerance of 10^{-6}. The bvp4c tool necessitates a preliminary assumption for Eqs (13)-(15) because the current problem may have multiple solutions. The assumption must preserve the behaviour of the solution and fulfill the boundary requirements in (16). Determining an initial guess for the first solution is not difficult

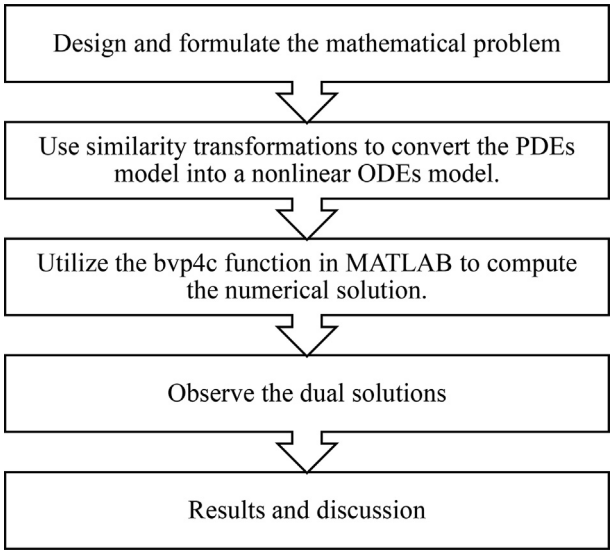

Fig. 2 Flow chart illustrating the mathematical solutions.

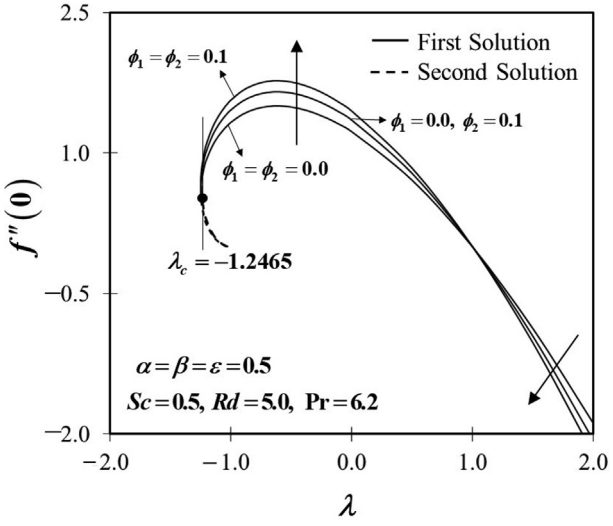

Fig. 3 $f''(0)$ with various values of ϕ.

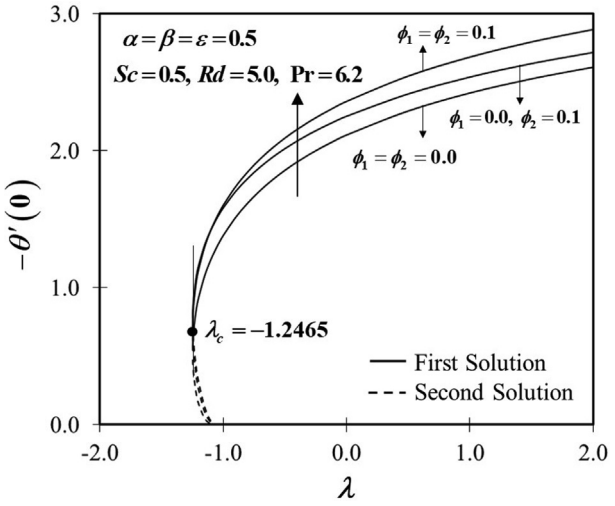

Fig. 4 $-\theta'(0)$ with various values of ϕ.

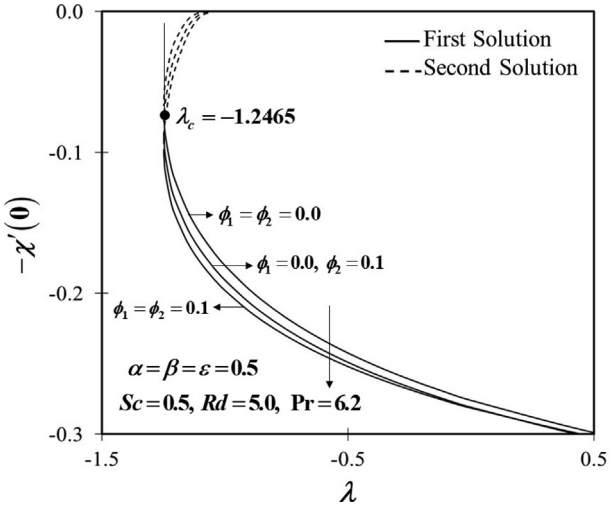

Fig. 5 $-\chi'(0)$ with various values ofϕ.

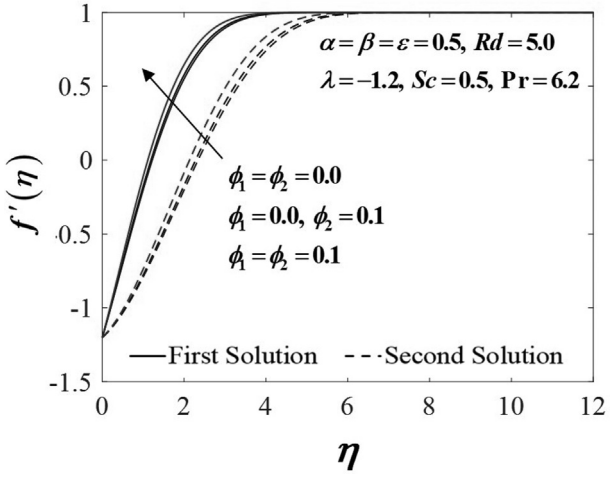

Fig. 6 $-f'(\eta)$ with various values of ϕ.

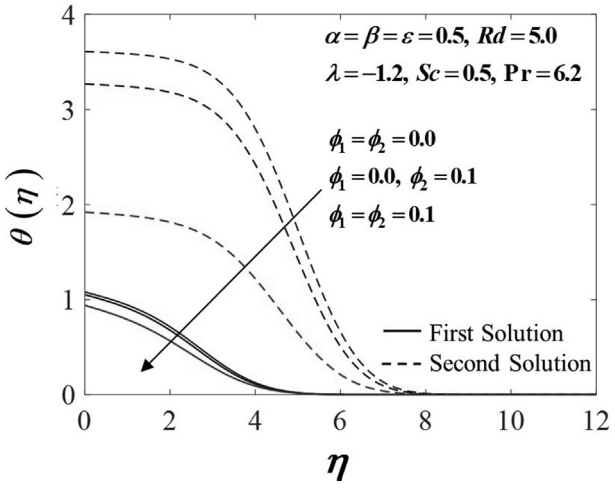

Fig. 7 $\theta(\eta)$ with various values of ϕ.

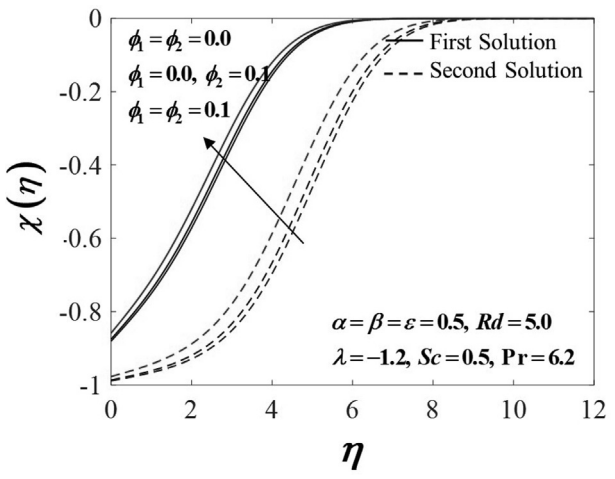

Fig. 8 $\chi(\eta)$ with various values of ϕ.

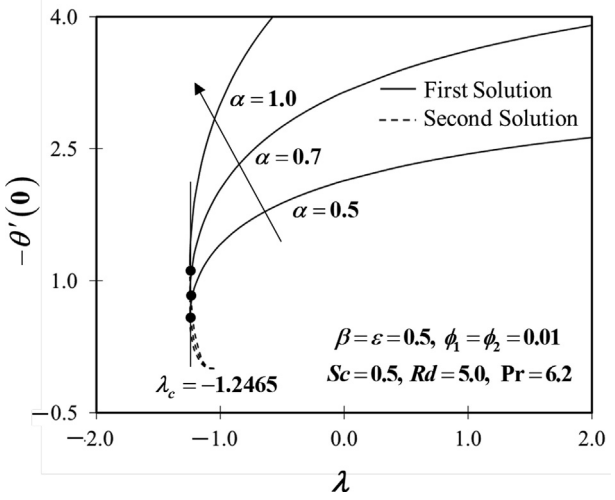

Fig. 9 $-\theta'(0)$ with various values of α.

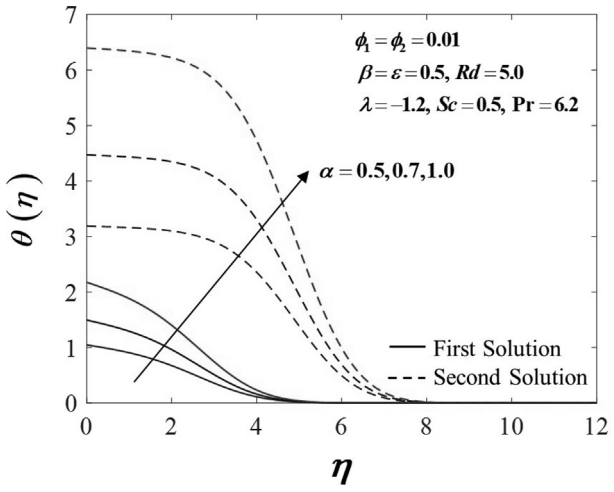

Fig. 10 $\theta(\eta)$ with various values of α.

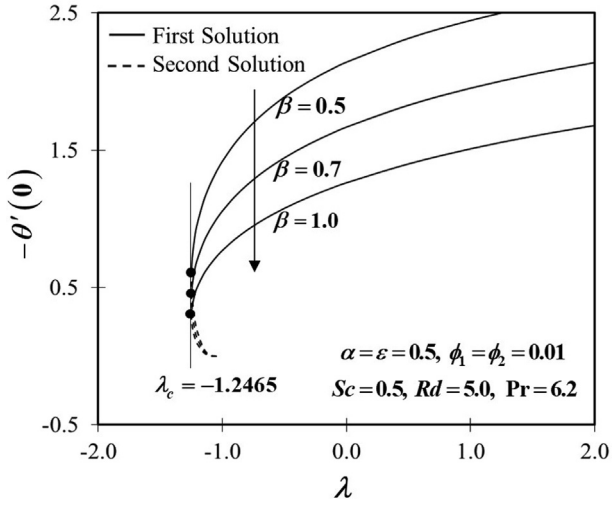

Fig. 11 $-\theta'(0)$ with various values of β.

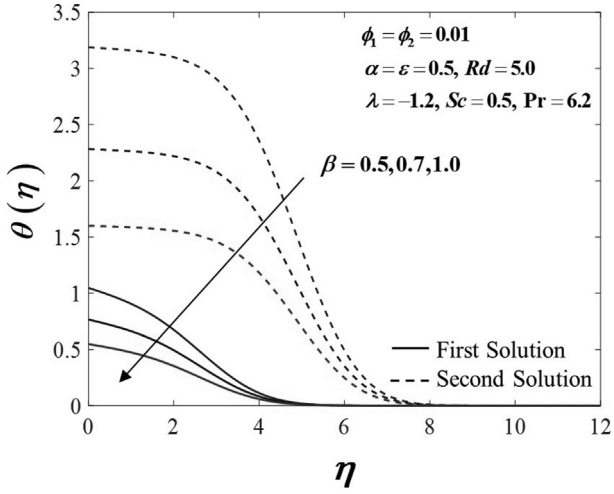

Fig. 12 $\theta(\eta)$ with various values of β.

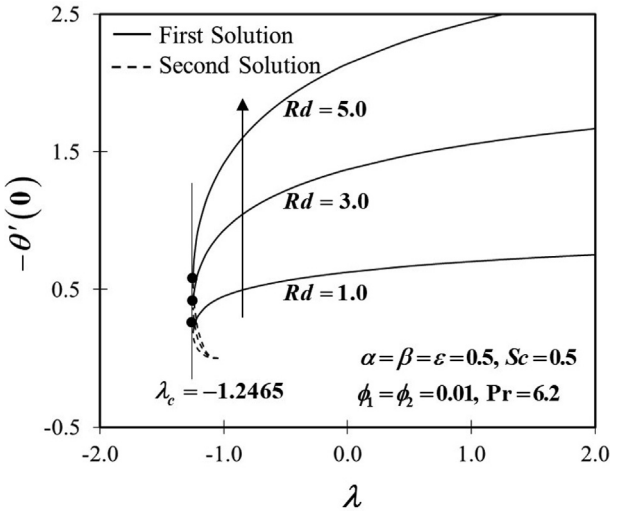

Fig. 13 $-\theta'(0)$ with various values of Rd.

Table 3 Model validation when $\phi_1=\phi_2=\alpha=\beta=\varepsilon=Sc=Rd=0$, Pr $=6.2$ and various λ.

λ	$f''(0)$		
	Wang [30]	Bachok et al. [53]	Current findings
2	–1.887310	1.887307	–1.887307
1	0.000000	0.000000	0.000000
0.5	0.713300	0.713295	0.713295
0	1.232588	1.232588	1.232588
–0.5	1.495670	1.495670	1.495670
–1	1.328820	1.328817	1.328817
–1.15	1.082230	1.082231	1.082231
–1.2	–	0.932473	0.932473
–1.2465	0.554300	0.584281	0.584281

because the bvp4c method will converge to the first solution even for poor guesses. The bvp4c technique will converge to the first solution even for bad guesses, therefore choosing a preliminary initial guess is straightforward for the first solution. Finding a second solution that is a sufficiently good guess is, however, fairly challenging. Hence, we applied the continuation strategy in this instance as pointed out by Shampine et al. [52]. The flow chart shown in Fig. 2 summarizes the solving method employed in this study.

In Figs. 3-13, the explanations of the generated flow and thermal behaviour of the problem are addressed and illustrated. By comparing the present study to prior reports, the validity of the study is verified. Table 3 displays the outcomes of model comparison for viscous fluid between the present results with Wang [30] and Bachok et al. [53]. In the meantime, Table 4 shows the validation results for Cu-H_2O nanofluids, while Table 5 indicates the results justification for Al_2O_3-H_2O nanofluids. It should be noticed that the results and findings exhibit good consistency as seen in Tables 3, 4, and 5, hence approving the mathematical formulation employed in this study. The current study emphasizes the existence of dual solutions in Figs. 3-13, due to the boundary condition's fulfil-

Table 4 Model validation when $\phi_1 = \alpha = \beta = \varepsilon = Sc = Rd = 0, \mathrm{Pr} = 6.2$ and various λ for $f''(0)$.

λ	$\phi_2 = 0.1$		$\phi_2 = 0.2$	
	Bachok et al. [53]	Current findings	Bachok et al. [53]	Current findings
2	–2.217106	–2.221631	–2.298822	–2.305321
1	0.000000	0.000000	0.000000	0.000000
0.5	0.837940	0.839650	0.868824	0.871281
0	1.447977	1.450932	1.501346	1.505590
–0.5	1.757032	1.760618	1.821791	1.826942
–1	1.561022	1.564208	1.618557	1.623133
–1.15	1.271347	1.273941	1.318205	1.321932
–1.2	1.095419	1.097655	1.135794	1.139004
–1.2465	0.686379	0.687783	0.711679	0.713692

Table 5 Model validation when $\alpha = \beta = \varepsilon = Sc = Rd = 0, \mathrm{Pr} = 6.2$ and various λ for $Re_x^{1/2} C_f$.

λ	ϕ_1	Yacob et al. [54]	Bachok et al. [53]	Current findings
–0.5	0.1	–	1.944000	1.946438
	0.2	–	2.497600	2.502748
0	0.1	1.601900	1.601900	1.604068
	0.2	2.058400	2.058400	2.062525
0.5	0.1	–	0.927100	0.928269
	0.2	–	1.191200	1.193577

ment in (16) as the parameters used are within the range of $0.5 \leqslant \alpha \leqslant 1.0$ (heat of reaction parameter), $0.5 \leqslant \beta \leqslant 1.0$ (reaction rate parameter), $1.0 \leqslant Rd \leqslant 5.0$ (thermal radiation parameter), $\varepsilon = 0.5$ (activation energy), and $\mathrm{Pr} = 6.2$ (Prandtl number for the water-based fluid). Meanwhile, the volumetric concentration of Al_2O_3-Cu/H_2O hybrid nanofluids is in the range of $0.00 \leqslant \phi_1, \phi_2 \leqslant 0.01$, or otherwise specified in the presented results.

The characteristics of the skin friction coefficient $f''(0)$, heat transfer rate $-\theta'(0)$, and mass transfer rate $-\chi'(0)$ behaviour to the nanoparticle volume concentration parameter can be observed in Figs. 3-5. The increment trend of the physical quantity $f''(0)$ is noticeable in the first solution of the shrinking sheet when the working fluid is shifted from viscous fluid $(\phi_{1,2} = 0.0)$ to Cu-H_2O nanofluids $(\phi_1 = 0.0,\ \phi_2 = 0.1)$ and Al_2O_3-Cu/H_2O hybrid nanofluids $(\phi_{1,2} = 0.1)$, as displayed in Fig. 3. This is because an increase in the volume fraction of nanoparticles causes the fluid's viscosity to rise. Meanwhile, a reduction pattern is observed in the first solution when the volume of nanoparticle concentration improved as the sheet is stretched. Fig. 4 demonstrates that as the volume concentration rises, the rate of heat transfer $-\theta'(0)$ increases. This best summarized that hybrid nanofluids exhibit excellent heat transfer performance, followed by nanofluid and viscous fluid. On the other hand, the behaviour of $-\chi'(0)$ which represents the rate of mass transfer at the surface declines when $\phi_{1,2}$ improves as portrayed in Fig. 5. This might occur because the mass transfer of the working fluids is accelerated by the volume concentration of nanoparticles, which lowers the rate of mass transfer at the surface.

The respective velocity, temperature distribution, and concentration profiles with the impact of $\phi_{1,2}$ parameter are presented in Figs. 6-8. All the solutions asymptotically fulfilled the far field boundary conditions up to boundary layer thickness $\eta_\infty = 12$, which affirms the results' validness, when the sheet is shrinking at $\lambda = -1.2$. Fig. 6 exhibits the increment of velocity profile $f'(\eta)$ in both solutions as the $\phi_{1,2}$ increased. The same behaviour is observed in the concentration profile $\chi(\eta)$, as presented in Fig. 8. However, a reversal outcomes is presented in Fig. 7, where the temperature profile $\theta(\eta)$ shows a downward trend with the escalation of the volume concentration of nanoparticles in the working fluid. This result is consistent with the behaviour of the heat transfer rate in Fig. 4, which was previously explained. It should be noticed that when the heat transfer rate rises, the temperature distribution falls. Based on the results generated in Figs. 3-8, the authors are clear that the percentage of nanoparticle concentration used for this specific computation is high. However, it is simply done to monitor how these three different working fluids respond. The nanoparticle concentration is then set to a total of 2% for the remaining of the investigation.

Additionally, Figs. 9 and 10 are supplied to provide insight into the effects of the heat of reaction α in hybrid nanofluids on the heat transfer rates and temperature profiles, respectively. The increment of $-\theta'(0)$ is observed as α increases (see Fig. 9), and also inclines the behaviour of $\theta(\eta)$ as in Fig. 10. This may be the result of Arrhenius kinetics working in conjunction with the radiation parameter, which causes internal heat conduction in the fluid and increases fluid velocity, raising the temperature profiles of the boundary layer over the shrinking surface. The impacts of the reaction rate parameter on the

rates of heat transfer and temperature profiles in hybrid nanofluids are depicted in Figs. 11 and 12, correspondingly. The downward trend of $-\theta'(0)$ is seen in Fig. 11 when β inclines and the temperature profile exhibits the same characteristic. Based on this results, it is clearly proven that higher value the reaction rate parameter ($\beta > 0.5$) may weaken the thermal performance of the particular problem. Thus, an appropriate values of β is encourage to ensure the efficiency of certain problem.

The influence of the thermal radiation impact Rd on $-\theta'(0)$, which rises as Rd intensifies, is seen in Fig. 13. The thermal radiation parameter is practically improved the heat transfer rate by increasing Rd, which also aids in transferring more heat into the fluid. This finding is significant because it shows that higher values of thermal radiation can enhance heat transfer efficiency. More heat will be produced and transferred into the flow as a result of the thermal radiation effect, increasing thermal performance. However, while it is recommended to employ the thermal radiation parameter with an acceptable value to prevent turbulent flow, it is noted that lowering this control parameter also helps to slow down the process of boundary layer separation. As a final remark, authors believe that in order to meet the demand for energy in the future, it is necessary to develop new adaptive nanofluids. However, compatibility issues provide a barrier to the development of the innovative hybrid nanofluids. Finding and creating a compatible hybrid nanocomposite is difficult because hybrid nanocomposites typically contain more than two different types of nanoparticles.

4. Conclusions

The present work highlights the effect of thermal radiation and Arrhenius kinetics in the case of hybrid nanofluid in the stagnation point flow. The Al_2O_3-Cu hybrid nanoparticles and H_2O as the based fluid are considered in the entire study. The formulated ordinary differential equation and specified boundary conditions generated from the similarity solutions are solved by employing the bvp4c solver in MATLAB software. The influences of some related govern parameters are pointed out. Our findings show that the hybrid nanofluid flow behaviour significantly enhances the system's ability to transfer heat, in comparison to viscous flow and nanofluid flow for this particular problem. Also, it is acknowledged that incorporating the nanoparticle volume concentration improves the heat transfer rate in this study. The flow and thermal progress of hybrid nanofluid are influenced by the heat of reaction and thermal radiation factors in the stagnation region. These two variables may assist in boosting the heat transfer rate of the current study. Meanwhile, the reaction rate parameter lowers the thermal efficiency of the hybrid nanofluid as the sheet stretches or shrinks. However, an appropriate value of this parameter may be adjusted to achieve the intended results. In overall results, dual solutions are obtained within the specific intervals of the physical parameters.

Declaration of Competing Interest

The authors declare that they have no known competing financial interests or personal relationships that could have appeared to influence the work reported in this paper.

Acknowledgements

This project is funded by *Publication Incentive Commendation Grant* from Universiti Teknikal Malaysia, Melaka (JURNAL/2020/FTKMP/Q00051). The authors appreciate the funding assistance provided by Universiti Teknikal Malaysia Melaka.

References

[1] K. Hiemenz, Die Grenzschicht an einem in den gleichförmigen Flüssigkeitsstrom eingetauchten geraden Kreiszylinder, Dinglers Polytech. J. 326 (1911) 321–324.
[2] E.R.G. Eckert, Die Berechnung des Warmeubergangs in der Laminaren Grenzschicht umstromter Korper, VDI Forschungsh. 416 (1942) 1–24.
[3] G.C. Dash, R.S. Tripathy, M.M. Rashidi, S.R. Mishra, Numerical approach to boundary layer stagnation-point flow past a stretching/shrinking sheet, J. Mol. Liq. 221 (2016) 860–866.
[4] M. Farooq, M.I. Khan, M. Waqas, T. Hayat, A. Alsaedi, M.I. Khan, MHD stagnation point flow of viscoelastic nanofluid with non-linear radiation effects, J. Mol. Liq. 221 (2016) 1097–1103.
[5] M.N. Rostami, S. Dinarvand, I. Pop, Dual solutions for mixed convective stagnation-point flow of an aqueous silica–alumina hybrid nanofluid, Chin. J. Phys. 56 (5) (2018) 2465–2478.
[6] M.I. Khan, S. Ullah, T. Hayat, M. Waqas, M.I. Khan, A. Alsaedi, Salient aspects of entropy generation optimization in mixed convection nanomaterial flow, Int. J. Heat Mass Transf. 126 (2018) 1337–1346.
[7] M.I. Khan, F. Haq, S.A. Khan, T. Hayat, M.I. Khan, Development of thixotropic nanomaterial in fluid flow with gyrotactic microorganisms, activation energy, mixed convection, Comput. Methods Programs Biomed. 187 (2020) 105186.
[8] M.I. Khan, A. Alsaedi, S. Qayyum, T. Hayat, M.I. Khan, Entropy generation optimization in flow of Prandtl-Eyring nanofluid with binary chemical reaction and Arrhenius activation energy, Colloids Surf. A: Physicochem. Eng. Asp. 570 (2019) 117–126.
[9] M.F. Javed, M.I. Khan, N.B. Khan, R. Muhammad, M. Ur Rehman, S.W. Khan, T.A. Khan, Axisymmetric flow of Casson fluid by a swirling cylinder, Results Phys. 9 (2018) 1250–1255.
[10] B. Mahanthesh, Statistical and exact analysis of MHD flow due to hybrid nanoparticles suspended in $C_2H_6O_2$-H_2O hybrid base fluid, in Mathematical Methods, in: Engineering and Applied Sciences, CRC Press, Boca Raton, 2020.
[11] B. Mahanthesh, Quadratic radiation and quadratic Boussinesq approximation on hybrid nanoliquid flow, in Mathematical Fluid Mechanics, De Gruyter, Berlin, 2021.
[12] B. Mahanthesh, Flow and heat transport of nanomaterial with quadratic radiative heat flux and aggregation kinematics of nanoparticles, Int. Commun. Heat Mass Transf. 127 (2021) 105521.
[13] K. Thriveni, B. Mahanthesh, Heat transport of hybrid nanomaterial in an annulus with quadratic Boussinesq approximation, Appl. Math. Mech. 42 (2021) 885–900.
[14] K. Thriveni, B. Mahanthesh, Sensitivity computation of nonlinear convective heat transfer in hybrid nanomaterial between two concentric cylinders with irregular heat sources, Int. Commun. Heat Mass Transf. 129 (2021) 105677.
[15] J. Mackolil, B. Mahanthesh, Optimization of heat transfer in the thermal Marangoni convective flow of a hybrid nanomaterial with sensitivity analysis, Appl. Math. Mech. 42 (11) (2021) 1663–1674.
[16] T. Gul, S. Nasir, S. Islam, S. Shah, M.A. Khan, Effective Prandtl number model influences on the $\gamma Al_2O_3\gamma Al_2O_3$–

H_2OH_2O and $\gamma Al_2O_3\gamma Al_2O_3$–$C_2H_6O_2C_2H_6O_2$ nanofluids spray along a stretching cylinder, Arab J. Sci. Eng. 44 (2019) 1601–1616.
[17] M. Muneeshwaran, G. Srinivasan, P. Muthukumar, C.C. Wang, Role of hybrid-nanofluid in heat transfer enhancement – A review, Int. Commun. Heat Mass Transf. 125 (2021) 105341.
[18] G. Huminic, A. Huminic, Entropy generation of nanofluid and hybrid nanofluid flow in thermal systems: A review, J. Mol. Liq. 302 (2020) 112533.
[19] S. Dinarvand, Nodal/saddle stagnation-point boundary layer flow of CuO–Ag/water hybrid nanofluid: a novel hybridity model, Microsyst. Technol. 25 (7) (2019) 2609–2623.
[20] I. Waini, A. Ishak, I. Pop, Hybrid nanofluid flow towards a stagnation point on a stretching/shrinking cylinder, Sci. Rep. 10 (2020) 1–12.
[21] N.S. Khashi'ie, N. Md Arifin, I. Pop, Mixed convective stagnation point flow towards a vertical Riga plate in hybrid Cu-Al_2O_3/water nanofluid, Mathematics 8 (2020) 912.
[22] N.A. Zainal, R. Nazar, K. Naganthran, I. Pop, Unsteady stagnation point flow of hybrid nanofluid past a convectively heated stretching/shrinking sheet with velocity slip, Mathematics 8 (2020) 1649.
[23] N.A. Zainal, R. Nazar, K. Naganthran, I. Pop, Stability analysis of unsteady hybrid nanofluid flow over the Falkner-Skan wedge, Nanomaterials 12 (2022) 1771.
[24] M. Imran, S. Yasmin, H. Waqas, S.A. Khan, T. Muhammad, N. Alshammari, N.N. Hamadneh, I. Khan, Computational Analysis of nanoparticle shapes on hybrid nanofluid flow due to flat horizontal plate via solar collector, Nanomaterials 12 (2022) 663.
[25] M.M. Bhatti, H.F. Öztop, R. Ellahi, I.E. Sarris, M.H. Doranehgard, Insight into the investigation of diamond (C) and silica (SiO_2) nanoparticles suspended in water-based hybrid nanofluid with application in solar collector, J. Mol. Liq. 357 (2022) 119134.
[26] N.A. Zainal, R. Nazar, K. Naganthran, I. Pop, Unsteady MHD hybrid nanofluid flow towards a horizontal cylinder, Int. Commun. Heat Mass Transf. 134 (2022) 106020.
[27] N.S. Khashi'ie, N.M. Arifin, M. Sheremet, I. Pop, Shape factor effect of radiative Cu–Al_2O_3/H_2O hybrid nanofluid flow towards an EMHD plate, Case Stud, Therm. Eng. 26 (2021) 101199.
[28] N.S. Wahid, N.M. Arifin, N.S. Khashi'ie, I. Pop, N. Bachok, M. E.H. Hafidzuddin, Flow and heat transfer of hybrid nanofluid induced by an exponentially stretching/shrinking curved surface, Case Stud, Therm. Eng. 25 (2021) 100982.
[29] E.G. Fisher, Extrusion of Plastics, Wiley, New York, 1976.
[30] C.Y. Wang, Stagnation flow towards a shrinking sheet, Int. J. Non. Linear. Mech. 43 (5) (2008) 377–382.
[31] N. Bachok, A. Ishak, I. Pop, Stagnation-point flow over a stretching/shrinking sheet in a nanofluid, Nanoscale Res. Lett. 6 (2011) 1–10.
[32] K. Bhattacharyya, G.C. Layek, Effects of suction/blowing on steady boundary layer stagnation-point flow and heat transfer towards a shrinking sheet with thermal radiation, Int. J. Heat Mass Transf. 54 (1-3) (2011) 302–307.
[33] I. Waini, I. Pop, S. Abu Bakar, A. Ishak, Stagnation point flow toward an exponentially shrinking sheet in a hybrid nanofluid, Int. J. Numer. Methods Heat Fluid Flow 32 (3) (2022) 1012–1024.
[34] M. Sajid, T. Hayat, Influence of thermal radiation on the boundary layer flow due to an exponentially stretching sheet, Int. Commun. Heat Mass Transf. 35 (3) (2008) 347–356.
[35] E.MA. Elbashbeshy, Radiation effect on heat transfer over a stretching surface, Can. J. Phys. 78 (12) (2000) 1107–1112.
[36] H. Waqas, S.A. Khan, T. Muhammad, N.M. Raza Shah Naqvi, Heat transfer enhancement in stagnation point flow of ferro-copper oxide/water hybrid nanofluid: A special case study, Case Stud, Therm. Eng. 28 (2021) 101615.
[37] M.F. Md Basir, J. Mackolil, B. Mahanthesh, K.S. Nisar, T. Muhammad, N.S. Anuar, N. Bachok, Stability and statistical analysis on melting heat transfer in a hybrid nanofluid with thermal radiation effect, Proc. Inst. Mech. Eng. Part E J. Process Mech. Eng. 235 (6) (2021) 2129–2140.
[38] A. Asghar, L.A. Lund, Z. Shah, N. Vrinceanu, W. Deebani, M. Shutaywi, Effect of thermal radiation on three-dimensional magnetized rotating flow of a hybrid nanofluid, Nanomaterials 12 (2022) 1566.
[39] A. Hassan, A. Hussain, M. Arshad, Q. Haider, A. Althobaiti, S. K. Elagan, M.S. Alqurashi, M.A.H. Abdelmohimen, Heat transport investigation of hybrid nanofluid (Ag-CuO) porous medium flow: Under magnetic field and Rosseland radiation, Ain Shams Eng. J. 13 (5) (2022) 101667.
[40] A. Saeed, M. Jawad, W. Alghamdi, S. Nasir, T. Gul, P. Kumam, Hybrid nanofluid flow through a spinning Darcy-Forchheimer porous space with thermal radiation, Sci. Rep. 11 (2021) 1–15.
[41] N.S. Wahid, N. Md Arifin, N.S. Khashi'ie, I. Pop, N. Bachok, M.E.H. Hafidzuddin, MHD mixed convection flow of a hybrid nanofluid past a permeable vertical flat plate with thermal radiation effect, Alexandria Eng J. 61 (4) (2022) 3323–3333.
[42] N.A. Zainal, R. Nazar, K. Naganthran, I. Pop, Unsteady flow of a Maxwell hybrid nanofluid past a stretching/shrinking surface with thermal radiation effect, Appl. Math. Mech. (English Ed.) 42 (10) (2021) 1511–1524.
[43] S.O. Salawu, E.O. Fatunmbi, S.S. Okoya, MHD heat and mass transport of Maxwell Arrhenius kinetic nanofluid flow over stretching surface with nonlinear variable properties, Results Chem. 3 (2021) 100125.
[44] N.S. Khan, Z. Shah, M. Shutaywi, P. Kumam, P. Thounthong, A comprehensive study to the assessment of Arrhenius activation energy and binary chemical reaction in swirling flow, Sci. Rep. 10 (2020) 7868.
[45] A. Shahid, H.L. Huang, M.M. Bhatti, M. Marin, Numerical computation of magnetized bioconvection nanofluid flow with temperature-dependent viscosity and Arrhenius kinetic, Math. Comput. Simul. 200 (2022) 377–392.
[46] M.B. Arain, M.M. Bhatti, A. Zeeshan, T. Saeed, A. Hobiny, Analysis of Arrhenius kinetics on multiphase flow between a pair of rotating circular plates, Math. Probl. Eng. 2020 (2020) 2749105.
[47] Z. Shah, A. Dawar, S. Nasir, S. Islam, W. Deebani, M. Shutaywi, Application of Arrhenius chemical process on unsteady mixed bio-convective flows of third-grade fluids having temperature-dependent in thermo-rheological properties, Waves Random Complex Media (2022) 1–20.
[48] J.H. Merkin, I. Pop, Stagnation point flow past a stretching/shrinking sheet driven by Arrhenius kinetics, Appl. Math. Comput. 337 (2018) 583–590.
[49] B. Takabi, S. Salehi, Augmentation of the heat transfer performance of a sinusoidal corrugated enclosure by employing hybrid nanofluid, Adv. Mech. Eng. 6 (2014) 147059.
[50] H.F. Oztop, E. Abu-Nada, Numerical study of natural convection in partially heated rectangular enclosures filled with nanofluids, Int. J. Heat Fluid Flow 29 (5) (2008) 1326–1336.
[51] S. Rosseland, Theoretical Astrophysics, Oxford University, New York, 1936.
[52] L. Shampine, J. Kierzenka, M. Reichelt, Solving boundary value problems for ordinary differential equations in MATLAB with bvp4c, Tutor, Notes 75275 (2000) 1–27.
[53] N. Bachok, A. Ishak, I. Pop, Stagnation-point flow over a stretching/shrinking sheet in a nanofluid, Nanoscale Res. Lett. 6 (2011) 623.
[54] N.A. Yacob, A. Ishak, I. Pop, Falkner-Skan problem for a static or moving wedge in nanofluids, Int. J. Therm. Sci. 50 (2) (2011) 133–139.